Weierstraß-Institut
für Angewandte Analysis und Stochastik

im Forschungsverbund Berlin e.V.

Preprint ISSN 0946 – 8633

Electronic structure and optoelectronic properties of strained InAsSb/GaSb multi quantum-wells

Thomas Koprucki[1], Michael Baro[1], Uwe Bandelow[1]

Tran Q. Tien[2], Fritz Weik[2], Jens W. Tomm[2],

Markus Grau[3], Markus-Christian Amann[3]

submitted: May 11, 2005

[1] Weierstraß-Institut
für Angewandte Analysis und Stochastik
Mohrenstrasse 39
10117 Berlin, Germany

[2] Max-Born-Institut
Max-Born-Strasse 2 A
12489 Berlin, Germany

[3] Walter Schottky Institut
Technische Universität München
Am Coulombwall 3
85748 Garching, Germany

No. 1028
Berlin 2005

2000 *Mathematics Subject Classification.* 82D37, 78A60.

Key words and phrases. Optoelectronic devices, light emitting devices, Indium-Arsenide-Antimonide, strained multi quantum-wells, photoluminescence measurements, absorption measurements, Stokes shift, **k·p** simulations.

Edited by
Weierstraß-Institut für Angewandte Analysis und Stochastik (WIAS)
Mohrenstraße 39
10117 Berlin
Germany

Fax: + 49 30 2044975
E-Mail: preprint@wias-berlin.de
World Wide Web: http://www.wias-berlin.de/

Abstract

A study of the optical properties of a set of $InAs_xSb_{1-x}/Al_{0.15}In_{0.85}As_{0.77}Sb_{0.23}/GaSb$ multiple quantum–wells ($0.82 < x < 0.92$) with built–in strains in the -0.62% to $+0.05\%$–range is presented. The energy of the lowest quantum–confined optical transition is calculated by $\mathbf{k}\cdot\mathbf{p}$–perturbation theory and experimentally determined by absorption measurements. Stokes shifts of photoluminescence, photocurrent and of the emission from light emitting devices against the absorption edge of the quantum–well are quantified. The impact of the decreasing carrier confinement in the $InAs_xSb_{1-x}$ quantum–well system with increasing mole fraction is analyzed theoretically, and experimentally demonstrated by photoluminescence measurements. Our results allow for the improvement of optoelectronic devices, in particular for tailoring emission spectra of light emitting diodes.

The $InAs_xSb_{1-x}$–system is the III–V–semiconductor alloy reaching the lowest direct band–gap value of all these materials ($\sim$ 100 meV). Therefore this particular mixed crystal system is of utmost interest for infrared (IR) optoelectronic applications such as heterostructure–based lasers and detectors [1,2]. For the purposes of device design and bandgap engineering quantitative knowledge on both, the intrinsic electronic structure but also on extrinsic effects such as broadening mechanisms, which eventually result in Stokes shifts of the emission, is required.

In this Letter we present the results of eight–band–$\mathbf{k}\cdot\mathbf{p}$–band structure calculations for strained $InAs_xSb_{1-x}$ multiple quantum–wells (MQW). The results, in particular the photon energy of the energetically lowest quantum–confined optical transition [3], are compared to the results obtained by transmittance, photoluminescence (PL), photocurrent and electroluminescence measurements at a set of 9 strained $InAs_xSb_{1-x}$ MQWs with various mole fractions x. The impacts of quantum–confinement, strain, and the observed Stokes shifts are separated from each other, quantified and discussed. Furthermore, our PL–data reflect the decreasing confinement energy for carriers in the wells with increasing mole fraction, which is also shown by our calculations. Thus our results involve the potential to improve optoelectronic devices, in particular light emitting diodes (LED).

The multi quantum well–samples consist of 10 $InAs_xSb_{1-x}$–wells and lattice matched $Al_{0.15}In_{0.85}As_{0.77}Sb_{0.23}$ barriers grown on 100–oriented GaSb–substrates. The As content variation of the MQWs from 0.82 to 0.92 results in a variation of the biaxial built–in strain from -0.62% (compression) to $+0.05\%$ (tension). The As content and the strain was determined by X–ray diffraction measurements. A 1μm $InAs_{0.895}Sb_{0.105}$–layer on GaSb is used as bulk–like reference. Test MQW LEDs are fabricated and analyzed as well.

All optical measurements are done by using a setup based on a Fourier–transform spectrometer BRUKER IFS 66v equipped with a PL–extension. For PL measurements the excitation wavelength is 1.064 μm. Technical details on the setup and the lock–in based PL–detection technique are given in Ref. 4. For the photocurrent measurements we use a STANFORD SR 570 as pre–amplifier before feeding the signal back into the spectrometer. PL–spectra are fitted to asymmetric Gaussians from which the value of the MQW–edge is extracted. This kind of technical fit refers to exponential tails of both, the thermal distribution at higher photon energies (Boltzmann–tail) and to the broadening (Urbach–tail) towards lower photon energies. The transmittance spectra are analyzed as follows. First the absorbance is calculated. Then the substrate–induced background, which is smooth, at least in the relevant 0.22–0.36 eV photon energy range, is eliminated by subtracting a 5^{th}–order polynomial. The result is then differentiated and the peak of the first derivative is identified with the MQW–edge [5]. If not indicated oterwise, all measurements are done at ambient temperature.

Theoretical analysis of the electronic band structure is done by means of eight–band–$\mathbf{k}\cdot\mathbf{p}$–perturbation theory which consistently models the band mixing between conduction and the valence bands including effects such as spin–orbit interaction and strain [6]. The structure of the corresponding Hamiltonians can be found in more detail in Ref. 7, their spectral properties are studied in Ref. 8. For eight–band–$\mathbf{k}\cdot\mathbf{p}$–Hamiltonians for heterostructures it is known that spurious solutions may pollute the band structure, if E_p/E

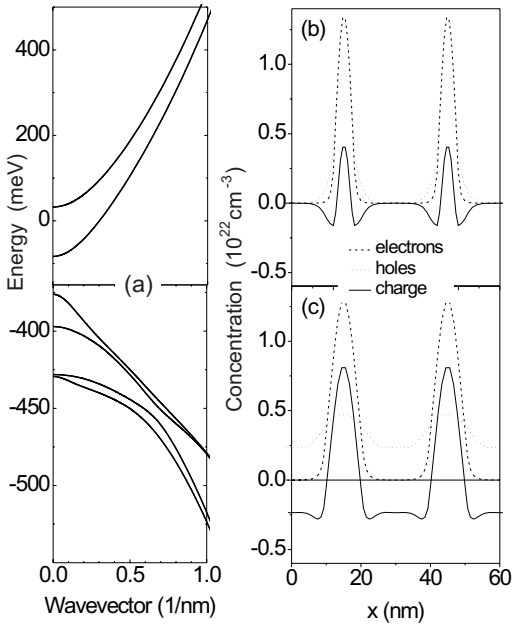

Figure 1: *Calculated conduction and valence band structures (a) of the sample with the As mole fraction of $x = 0.82$ at ambient temperature. (b) Local carrier density distribution in the MQW–region of the sample with $x = 0.82$ for a sheet density $n = p = 10^{11}\mathrm{cm}^{-2}$. The dashed line represents the electron density n, the dotted line gives the hole density p, and the solid one the charge density $n - p$. (c) Local carrier density distribution in the MQW–region of sample 0.92 for a sheet density $n = p = 10^{11}\mathrm{cm}^{-2}$. The dashed line represents the electron density n, the dotted line gives the hole density p, and the solid one the charge density $n - p$.*

exceeds a critical value, which is the case in our low gap material, see Refs. 9 and 10. We overcome this problem by a proper rescaling of E_p. Here E_p is the optical matrix element defined by the Kane parameter P, which serves as a measure of the coupling between valence and conduction bands, and E is the MQW–edge. Our simulation parameters are taken from Ref. 11 according to the ternary and quaternary interpolation schemes described there [12]. The band gap and the spin–split–off energy are obtained by means of quadratic interpolation, whereas the remaining material parameters are obtained by linear interpolation. For the calculations the in–plane strain is determined by $\epsilon_{xx} = \epsilon_{yy} = (a_0 - a)/a$, where $a_0 = 0.6096\,\mathrm{nm}$ is the lattice constant of the GaSb substrate, and a is the lattice constant of the corresponding layer material. Figure 1 (a) shows the results of the calculation of the conduction (top) and valence band (bottom) structures of the sample with $x = 0.82$. Such analysis is done for all samples in the 0.82–0.92 mole fraction range and the calculated MQW–edge is found to vary linearly with a slope $\mathrm{d}E/\mathrm{d}\epsilon = 8.4\,\mathrm{eV}$ or $\mathrm{d}E/\mathrm{d}x = 571\,\mathrm{meV}$ (blue shift). Extra calculations are made for the separation of the impacts of strain and mole fraction. The pure strain results in a $\mathrm{d}E/\mathrm{d}\epsilon = -1.34\,\mathrm{eV}$ or $\mathrm{d}E/\mathrm{d}x = -91\,\mathrm{meV}$ contribution to the slope (IR-shift) indicating reduced compression for larger mole fractions.

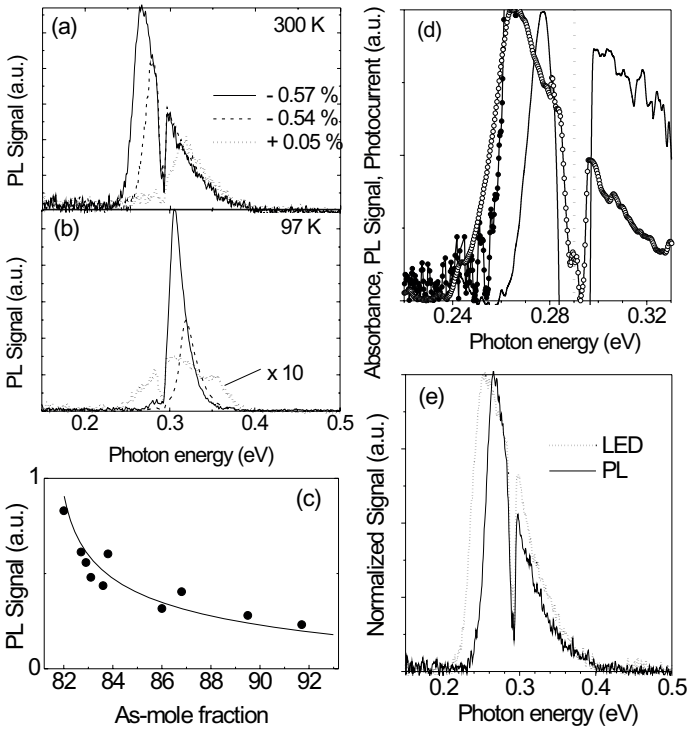

Figure 2: *Optical spectra. (a) Selected PL spectra at ambient and (b) at $T = 97\,\mathrm{K}$. (c) Room–temperature PL intensities versus As- mole fraction. (d) PL (open circles), absorbance (full line) and photocurrent (full circles) spectra from an $InAs_{0.82}Sb_{0.18}/Al_{0.15}In_{0.85}As_{0.77}Sb_{0.23}/GaSb$ multiple quantum–well sample. (e) Comparison between LED–emission and PL obtained from an $InAs_{0.82}Sb_{0.18}/Al_{0.15}In_{0.85}As_{0.77}Sb_{0.23}/GaSb$ LED.*

Moreover we analyze the local charge density distributions within an extract of the complete MQW–structures for two samples representing the borders of the mole fraction range analyzed, namely $x = 0.82$ and 0.92. This is shown in Figs. 1 (b) and (c), respectively. In accordance with data obtained from electrical transport measurements we assume charge neutrality with sheet densities of $n = p = 10^{11}\mathrm{cm}^{-2}$. For the sample with $x = 0.82$ (compressive strain), see Fig. 1 (b), we see efficient confinement of both, the electrons and the holes. The valence band offset amounts to 54 meV. Thus the density of unconfined carriers remains small and therefore screening effects are not expected to be prominent. For the tensile strained sample with $x = 0.92$ the result is quite different; see Fig. 1 (c). The valence band offset of 13 meV only indicates a tendency towards hole de–confinement. Since the electrons are still well–confined, the delocalization of the holes results in a substantially increased net charge density. Reduced wave–function overlap and additional screening are both expected to result eventually in poorer PL.

Now spectroscopic data are presented. In Fig. 2 (a) and (b) we show typical PL–spectra of selected samples. Note the pronounced CO_2–absorption line. As expected the PL blue–shifts with increasing As–mole fraction. The sample with $x = 0.92$ appears

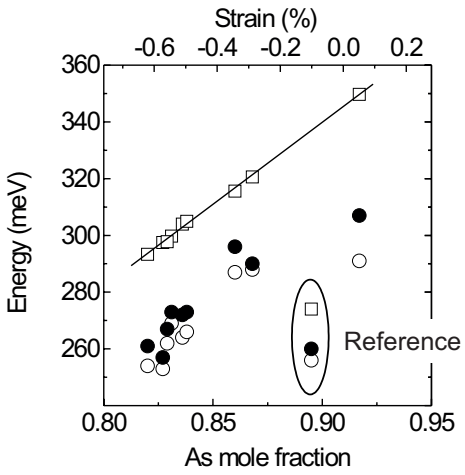

Figure 3: *Comparison between* $\boldsymbol{k}\cdot\boldsymbol{p}$*–band structure calculations and experiments. Full circles indicate the MQW–edge as determined from transmittance, whereas open circles point to the edge as deduced from PL. Squares mark the edge as obtained from the energy difference of the lowest conduction band subband (at* $k = 0$*) and the highest valence subband (at* $k = 0$*) according to 8–band* $\boldsymbol{k}\cdot\boldsymbol{p}$*–calculations for the full MQW–structures, with parameters from Vurgaftman et al., see Ref. 11 inclusively bowing. Note that calculations on single quantum wells provide almost the same results.*

rather smeared and shows the poorest ambient–temperature PL. For lowered temperature, this special behavior becomes even more pronounced; see Fig. 2 (b). From Fig. 2 (c) it becomes clear that this finding is in accordance with a general trend. Therefore we assume the poorer PL towards larger As–mole fractions to be caused by increasing carrier delocalization. Obviously, this effect is stronger than the potential benefits for the PL–signal which might arise from increasing Auger–lifetimes for larger As–mole fractions as theoretically predicted [13].

Fig. 2 (d) exemplarily shows spectra monitored from the compressive strained sample with $x = 0.82$. The tendency represented by this figure, however, is quite typical for all our samples. Between the MQW–edge determined from absorbance data on the one side and PL and photocurrent spectra on the other side there is a systematic Stokes–shift. For the magnitude of the Stokes–shift we see no clear tendency within the mole–fraction range covered by our study. The average value amounts to (7 ± 4)meV. Fig. 2 (e) now demonstrates that the Stokes–shift becomes even larger if the electroluminescence from a LED is considered. A ~ 15 meV shift with respect to the PL, which is already Stokes-shifted with respect to the MQW absorption edge, see Fig. 2 (d), is seen. Obviously localized carriers contribute to the LED–emission. Consequently, a rather large Stokes-shift of the emission, in this particular case 7 meV + 15 meV = 22 meV, is to be taken into account for device design purposes. We should note that this finding contradicts the results published by Kurtz et al., who observed the PL peak to be 8 meV below the LED-emission [14]. A detailed analysis of the mechanisms responsible for the observed

Stokes–shifts is beyond the scope of this letter; however, thickness fluctuations within the MQW–system as well as alloy fluctuations are likely microscopic sources.

Finally, we directly compare our theoretical findings with the data obtained for different mole fractions; see Fig. 3. At the top abscissa we represent the built–in strain, which is, at least for our particular MQW design, a dependent parameter only. When comparing "theory" and "experiment" it is obvious that the experimental data are energetically below the calculated results. In cases of PL, photocurrent and electroluminescence data this fact is already discussed within the framework of carrier localization effects. The transmittance data, however, are expected to give rather straight access to the intrinsic band structure. Thus we have to state a systematic (32 ± 7)meV IR-shift of the QW–edge data as determined by absorption compared to the theory. For device design purposes this discrepancy must be taken into account. We should mention that this tendency holds even for the $InAs_{0.895}Sb_{0.105}$ bulk–like sample; see Fig. 3. [15,16] Thus it is not likely to be a residual effect of our $\mathbf{k}\cdot\mathbf{p}$ calculation. This reference sample also allows a comparison between "bulk" and MQW. The $InAs_{0.895}Sb_{0.105}$ "bulk" sample shows edges at 260meV and 256 meV as obtained by transmittance and PL, respectively. Interpolating the transmittance and PL data of the MQW with a mole fraction closeby $InAs_{0.895}Sb_{0.105}$ we find a 40meV blue shift of the MQW data. This shift represents the total of the contributions from quantum confinement and strain.

Summarizing, we present a complementary study of selected optoelectronic properties of a set of $InAs_xSb_{1-x}/Al_{0.15}In_{0.85}As_{0.77}Sb_{0.23}$/GaSb MQWs ($0.82 < x < 0.92$) with built–in strains in the -0.62% to $+0.05\%$–range. The energy of the lowest MQW–transition is theoretically calculated and experimentally determined by absorption measurements. Stokes shifts of PL, photocurrent and LED–emission are quantified. We find decreasing confinement for carriers in the wells with increasing mole fraction or lowering of compressive strain. This is also shown by our calculations. Our results allow for the improvement of optoelectronic devices, in particular for tailoring LED emission spectra.

Acknowledgments. The work is funded in part by the German Bundesministerium für Bildung und Forschung under grant 03 N1084. Thomas Koprucki is supported by the DFG Priority Program Analysis, Modeling and Simulation of Multiscale Problems under Grant FU 316/5-2 and Michael Baro is supported by the DFG research center Matheon in Berlin.

References

[1] A. Wilk, M. El Gazouli, M. El Skouri, P. Cristol, P. Grech, A. N. Baranov, and A. Joullie, *Appl. Phys. Lett.* 77, pp. 2298 (2000).

[2] H. H. Gao, A. Krier, and V. V. Sherstnev, *Appl. Phys. Lett.* 77, 872 (2000).

[3] We will refer to this energy as the MQW-edge.

[4] F. Weik, J. W. Tomm, R. Glatthaar, U. Vetter, D. Szewczyk, J. Nurnus, A. Lambrecht, M. Grau, R. Meyer, M.–C. Amann, B. Spellenberg, M. Bassler, *SPIE Proc.* 5366, pp. 149 (2004).

[5] This straightforward approach ensures the determination of the correct value assuming a step–like combined density of states and the action of symmetric broadening mechanisms, only.

[6] http://www.wias-berlin.de/software/qw/

[7] P. Enders, A. Bärwolff, M. Woerner, and D. Suisky, *Physical Review B* 51, pp. 16695 (1995).

[8] U. Bandelow, H.-Chr. Kaiser, T. Koprucki, and J. Rehberg, *Numerical Functional Analysis and Optimization* 21, pp. 379, (2000).

[9] B. A. Foreman, *Phys. Rev. B* 56, pp. 12748 (1997).

[10] X. Cartoixa Soler, *Theoretical Methods for Spintronics in Semiconductors with Applications*, chapter 6 together with section 5.3.2. PhD Thesis, California Institute of Technology, Pasadena, California, USA, 2003. Online available: http://resolver.caltech.edu/CaltechETD:etd-05232003-104331.

[11] I. Vurgaftman, J. R. Meyer and L. R. Ram-Mohan, *J. Appl. Phys.* 89, pp. 5815 (2001).

[12] In all cases we chose those parameters given as by Ref. 11 as "recommended" ones.

[13] A. Rogalski and Z. Orman, *Infrared Phys.* 25, pp. 551 (1985).

[14] S. R. Kurtz, R. M. Biefeld, L. R. Dawson, K. C. Baucom, and A. J. Howard, *Appl. Phys. Lett.* 64, pp. 812 (1994).

[15] The band gap for the ternary bulk–like sample is calculated with the same quadratic interpolation scheme and the same parameters from Ref. 11 used in the barriers and wells of the MQW structures. The band gap alternation by the weak compressive strain is taken into account according to Ref. 16.

[16] C. G. Van de Walle, *Phys. Rev. B* 39, pp. 1871 (1989).